Estonian Journal of Ecology, 2008, **57**, 3, 185–197 doi: 10.3176/eco.2008.3.02

Optical and physical properties of coastal water and their relations to radar (ASAR) data – a case study of Muuga Bay, Gulf of Finland

Liis Sipelgas✉, Urmas Raudsepp, and Rivo Uiboupin

Marine Systems Institute, Tallinn University of Technology, Akadeemia tee 21B, 12618 Tallinn, Estonia

✉ Corresponding author, liis@sea.ee

Received 18 December 2007, in revised form 18 April 2008

Abstract. A field study of optical and physical properties in Muuga Bay, Gulf of Finland, was performed on 30 May 2007. In one of the studied stations traces of ballast water were visible on the water surface. An Advanced Synthetic Aperture Radar (ASAR) image was received and analysed from the same area. The vertical profiles of the absorption and attenuation coefficients together with the temperature and salinity profiles were measured in 13 stations. The concentrations of oil products, chlorophyll *a*, coloured dissolved organic matter, and suspended particulate matter were determined from water samples. The spatial distribution of temperature, salinity, and optically active substances indicated four distinct areas: the southern coastal area with saline, cold, and chlorophyll *a* poor upwelling water; the western coast of the bay with warmer and chlorophyll *a* richer surface water; open water dominated by higher concentrations of coloured dissolved organic matter; and Muuga harbour where the water had a high concentration of suspended particulate matter and chlorophyll *a*, which caused stronger light attenuation and a thinner euphotic layer compared to the other parts of the bay. Regression analysis showed that the absorption coefficient at 676 nm correlated well with the chlorophyll *a* concentration and the scattering coefficient at 555 nm correlated with the suspended matter concentration in Muuga Bay. The correlation coefficient between ASAR data and oil products was 0.71 although the concentration of oil products was relatively low (0.01–1.72 ppm).

Key words: Gulf of Finland, Muuga Bay, optical properties of water, radar (ASAR).

INTRODUCTION

Among various human activities the development of harbours and increasing ship transport have a potential impact on the ecological state of coastal waters in the Baltic Sea. The ecological state of coastal waters is influenced by an increasing amount of suspended particulate matter (SPM) released into the water environment during dredging and dumping (Erftemeijer & Lewis., 2006; Sipelgas et al., 2006). In the Gulf of Finland, the probability of oil spills is high due to the increasing oil transportation. Several oil pollution incidents happened in the gulf over the last decade. Direct environmental impacts of oil spills affect seabirds and coastal ecology especially when the spill hits the shore. To minimize the negative effect of

oil pollution and to facilitate fast application of oil combating methods an early detection of oil spills at sea is of a great importance.

Many studies have proved that radar images can provide information on possible location and extent of oil spills (Gade & Alpers, 1999; Solberg et al.,1999; Brekke & Solberg, 2005; Topouzelis et al., 2007). Distinguishing between oil pollution and natural phenomena from a radar image is a complicated task, especially so in the case of coastal waters. Various physical and biological phenomena such as low wind areas, upwelling zones, internal waves, natural organic films, and phytoplankton accumulations, can cause structures looking like an oil spill on radar images. Some of these natural phenomena can be detected by passive remote sensing or by field measurements of physical and optical properties of water.

The aim of the current study was to investigate the relationships between the attenuation, absorption, and scattering coefficients and the concentrations of chlorophyll *a* (Chl *a*), SPM, dissolved organic matter (CDOM), and oil products. Regression analysis between radar (ASAR, Advanced Synthetic Aperture Radar) images and possible sources of look-alikes was performed. This case study focuses on Muuga Bay, a semi-enclosed bay in the southern Gulf of Finland, where biological productivity is relatively high and anthropogenic impacts caused by intensive ship transport and harbour development are increasing.

METHODS

Field measurements were made on 30 May 2007 between 11 a.m and 16.00 p.m. The locations of the sampling stations are shown in Fig. 1. According to the HILRAM model, the winds from the east were 4–6 m s^{-1} on Muuga Bay. A thin organic film, probably caused by ballast water, was visible on the water surface in station 18 during sampling.

In situ measurements

The vertical profiles of attenuation and absorption coefficients were measured by an ac-9 instrument (attenuation and absorption meter manufactured by WET Labs Inc). The system was calibrated based on the Wet Labs user manual. The absorption values were corrected for temperature and light scattering. The vertical profiles of temperature and salinity were measured by SeaBird CTD.

Laboratory analysis

The concentration of Chl *a* (C_{chl}, in mg m^{-3}) was determined by filtering the water samples through Whatman GF/C glass microfibre filters (pore size 1.2 μm, diameter 47 mm; Whatman International Ltd., Maidstone, England), extracting the pigments with ethanol and measuring the absorption at the wavelengths of 665 nm and 750 nm. The values of C_{chl} were calculated using the Lorenzen (1967) formula.

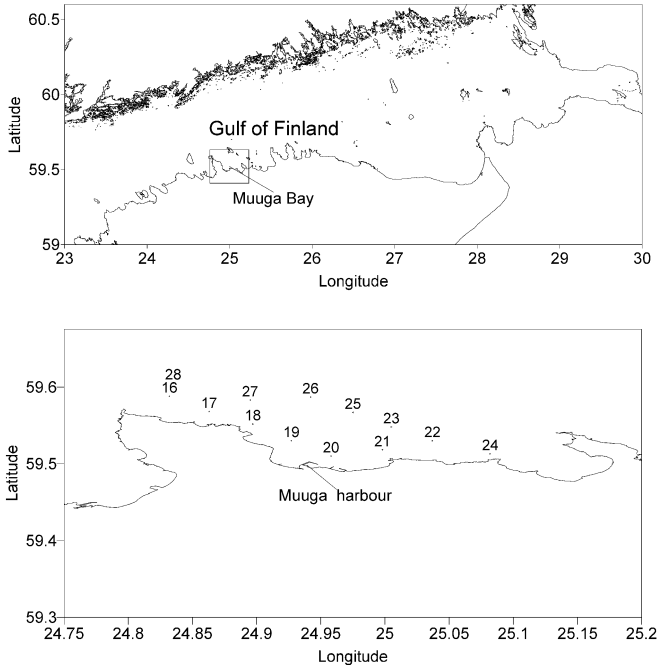

Fig. 1. Locations of the sampled stations in Muuga Bay.

The dry weight method was used to determine the concentration of SPM. Samples were filtered through pre-weighed Millipore membrane filters (pore size 0.45 μm, diameter 47 mm; Millipore Corporation, Bedford, MA) and the filters were dried to a constant weight at a fixed temperature (103–105 °C). The increase in the filter weight shows the suspended matter concentration in the water sample.

The spectrometric attenuation coefficient of filtered water ($c_f^*(\lambda)$) can be used to describe the content of CDOM. Water samples were filtered through Millipore membrane filters (pore size 0.45 μm, diameter 47 mm; Millipore Corporation, Bedford, MA) and the corresponding attenuation spectra were determined from filtered water using a laboratory spectrophotometer *Helios* γ. The concentration of CDOM was calculated according to Højerslev (1980):

$$C_{\mathrm{CDOM}} = \frac{c_f^*(\lambda)}{\exp(-S(\lambda-\lambda_0))\cdot a_{\mathrm{CDOM}}^*(\lambda_0)}, \tag{1}$$

where $a_{\mathrm{CDOM}}^*(\lambda_0)$ is specific absorption coefficient of dissolved organic matter, whose numerical value at $\lambda_0 = 380$ nm was taken equal to 0.565 $\mathrm{Lm^{-1}\ mg^{-1}}$

(Højerslev, 1980); S is the slope parameter equal to 0.017 nm^{-1} (Sipelgas et al., 2003); $c_f^*(\lambda)$ was taken from the spectrometrical reading at $\lambda = 380$ nm.

The concentration of oil products was determined by gas chromatography in the laboratory of the Estonian Environmental Research Centre.

SAR image

The ENVISAT SAR Wide Swath Product with 75 m pixels spacing from 30.05.2007, 11.45 a.m. was provided by KSAT (Kongsberg Satellite Services). The wind conditions were good (wind speed up to 7 m s^{-1}), therefore the rate of speckled noise was minimal. For the reduction of noise a 3 by 3 Local Sigma filter was implemented on the image. Georeferencing of image pixels was carried out before the backscatter values were obtained from a single polarization (transmitted – vertical component of signal, received – vertical component of back-scattered signal) ground range multi-look image.

RESULTS AND DISCUSSION

The surface temperature varied between 4.5 and 10.1 °C in Muuga Bay on 30 May (Table 1), which is a wide range for the small area that was covered by the measurements. The highest temperature of 10.13 °C was measured in station 18 where ballast water was visible on the surface. So, the local temperature maximum around that station was most likely caused by the higher temperature of the bilge

Table 1. The concentrations of chlorophyll *a*, suspended particulate matter, coloured dissolved organic matter, and oil products and the measured surface temperature and salinity

Station	Chl, μg L^{-1}	SPM, mg L^{-1}	CDOM, mg L^{-1}	Oil products, ppm	Temperature, °C	Salinity
16	3.57	2.6	3.80	n.d.	8.08	5.54
17	5.24	4	2.57	n.d.	9.16	5.55
18	5.00	5.8	3.30	1.18	10.13	5.54
19	3.57	3.4	2.73	0.46	7.86	5.57
20	5.71	5.4	3.34	1.72	8.50	5.61
21	3.09	3.6	3.79	1.4	6.90	5.58
22	3.09	3.6	3.26	n.d.	8.39	5.50
23	3.81	3.4	4.81	n.d.	7.17	5.43
24	2.14	5.6	n.d.	0.01	4.54	5.72
25	4.05	3.2	4.20	0.51	8.33	5.38
26	3.33	4.2	3.18	n.d.	7.79	5.36
27	4.05	4	4.48	1.07	8.71	5.41
28	3.33	3.4	3.99	0.76	8.80	5.48

n.d., not detected.

water. The lowest temperatures were measured in the southern coastal area of the bay. The surface salinity varied between 5.38 and 5.72 (Table 1). The salinity values were the highest in stations 20, 21, and 24. In general, the area with low temperature matches the area with higher salinity. The wind from the east favours upwelling of cold and saline water at the coast of the southern bay. Upwelling is visible at the outreaching part of the coastline (stations 21 and 24) and is highly variable in space. Due to moderate wind conditions and complex coastline, the upwelling signature is detectable either in temperature or salinity values over the narrow strip of coastal water.

The concentrations of Chl *a*, SPM, CDOM, and oil products are given in Table 1. The concentration of Chl *a* was from 2.14 to 5.71 μg L^{-1}. The end of May in the Gulf of Finland can be described as the relaxation period after spring bloom. The Chl *a* values were higher in the stations located near the western coast of Muuga Bay. The lowest values were measured in the stations where upwelling was detectable. The distribution of Chl *a*, temperature, and salinity indicates that surface water of the bay was transported to the west and northwest by the wind from the east. At the southern coast of the bay the surface water was then replaced by cold, saline, and low Chl *a* water from deeper layers. The concentrations of SPM varied between 2.6 and 5.8 mg L^{-1}. The highest value (5.8 mg L^{-1}) was measured in station 18, where a film of bilge water was seen on the water surface. Higher SPM concentrations were also seen in the harbour (station 20) and in the most pronounced upwelling location (station 24). The former can be explained by harbour operation, while the latter can be explained by resuspension of sediments due to wave and current action close to the coast. The concentration of CDOM varied from 2.57 to 4.81 mg L^{-1}. In general, higher concentrations of CDOM were detected at the stations that are located in the open part of the bay. The concentration of oil products was over 1 ppm in stations 18, 20, 21, and 27. Stations 20 and 21 were the closest to the harbour and in station 18 bilge water was seen on water surface. Also, station 27 was close to the area where bilge water was detected. In other sampled stations the concentration of oil products was less than 1 ppm.

The spectra of attenuation, absorption, and scattering coefficients at a depth of 0.5 m are shown in Figs 2a,c,d and the ratio of the absorption coefficient to the scattering coefficient is shown in Fig. 2b. The spectral shape of the scattering coefficient is similar for all stations having a maximum at 510 nm (Fig. 2c). The variation of the absorption coefficient is relatively small – from 1.5 to 1.8 at a wavelength of 412 nm – and its spectral shape does not differ much between the stations (Fig. 2d). The attenuation coefficient at 412 nm varied between 1.9 and 3.65 m^{-1}. In stations 20, 18, 17, and 24 the attenuation and scattering coefficients were higher compared to the other stations. In station 20 scattering dominated over absorption in the whole range of the spectrum (Fig. 2b). Scattering was higher than absorption in stations 17, 18, and 24, except at a wavelength of 412 nm. The high attenuation coefficient in these stations can be explained by relatively higher concentrations of optically active substances than in the other stations.

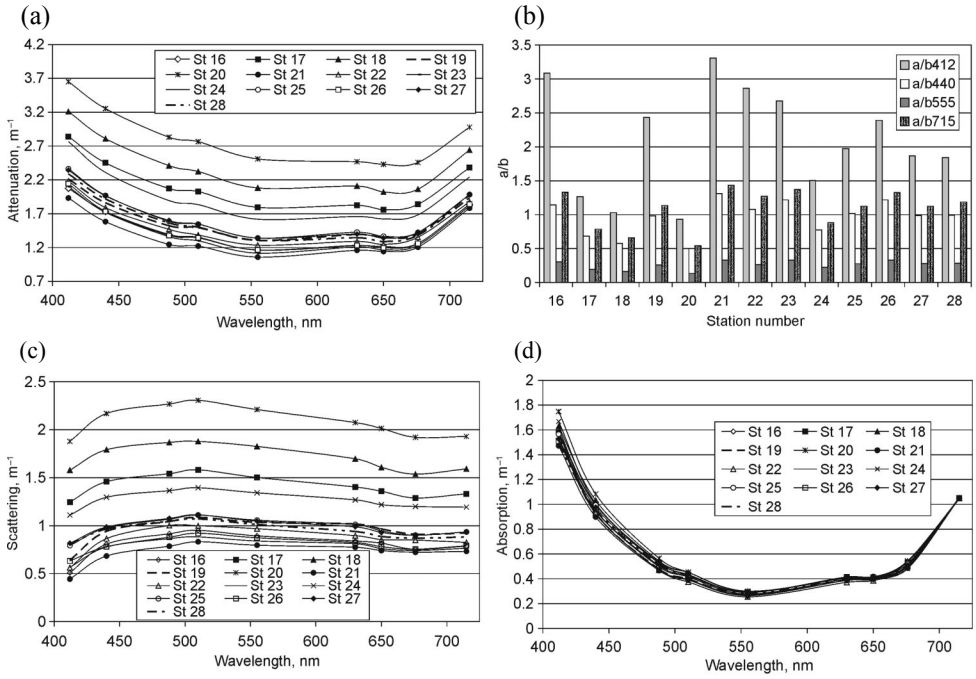

Fig. 2. (a) Attenuation coefficient in the stations at 0.5 m depth; (b) ratio of the absorption to scattering coefficient at wavelengths 412, 440, 555, and 715 nm; (c) scattering coefficient in the stations at 0.5 m depth; (d) absorption coefficient in stations at 0.5 m depth.

The concentrations of Chl *a* and SPM were high in stations 20 and 18. In station 17 the Chl *a* concentration was also high, but the SPM concentration was moderate. In station 24 only the SPM concentration was high. In stations 16, 21, 22, and 23, where the values of attenuation were the smallest (Fig. 2a), absorption was more than 2.5 times higher than scattering at a wavelength of 412 nm (Fig. 2b). The opposite result was earlier obtained in Estonian north-western coastal waters where scattering dominated over absorption (Sipelgas et al., 2004).

Linear relationships between the absorption/scattering coefficients and concentrations of SPM/Chl *a* were calculated using the measured data. A linear correlation between the absorption coefficient at 676 nm and Chl *a* concentration in water was found in several studies (e.g. Claustre et al., 2000; McKee et al., 2003). According to this study, there was a significant linear relationship between the absorption coefficient at 676 nm and the concentration of Chl *a* for the surface water in Muuga Bay:

$$C_{\text{chl}} = 48.737 \times a(676) - 21.064,\ R = 0.94,\ p = 9.7 \times 10^{-6},\ n = 13. \qquad (2)$$

No linear relationship was found in the coastal water of north-western Estonia (Sipelgas et al., 2004). This disparity may be explained by the fact that the measure-

ments in the north-western Estonian coastal sea were carried out at the end of July/beginning of August when different phytoplankton species dominate.

Scattering is known to be a proxy for the SPM content in water. Herlevi (2002) found a correlation ($R = 0.85$) between the average total scattering (over the ac-9 wavelengths) and the concentration of SPM for Finnish and Estonian lakes. In an earlier study (Sipelgas et al., 2006) we found a correlation ($R = 0.55$) between the SPM concentration (C_{SPM} mg L^{-1}) and scattering coefficient at a wavelength of 715 nm. For Muuga Bay, the best correlation was between the scattering coefficient at 555 nm and C_{SPM} with the corresponding linear regression formula:

$$C_{SPM} = 1.81 \times b(555) + 1.87,\ R = 0.78,\ p = 0.006,\ n = 13. \quad (3)$$

Regression formulas (2) and (3) were used to calculate the vertical profiles of C_{Chl} and C_{SPM} down to 12 m depth. The four representative profiles of C_{Chl} and C_{SPM} for stations 17, 18, 20, and 24 are shown in Fig. 3. In station 20, which was the closest to the Muuga harbour, the estimated C_{Chl} decreased monotonically from 6 to 3 mg m^{-3} at 11 m depth and then a sharp drop to a value of 1 mg m^{-3} followed. The SPM concentration was nearly homogeneous between 5 and 6 mg L^{-1} down to 11 m depth. In station 17 the C_{Chl} value was high like in station 20, but the upper layer extended down to 6 m depth only. Even so the SPM profile is similar to the Chl *a* profile and the concentrations of SPM remain between 4 and 4.5 mg L^{-1} in the upper layer. Comparison of the absolute values in stations 17 and 20 reveals that while SPM contains both phytoplankton and mineral particles, the SPM in station 17 contains relatively more phytoplankton particles. In stations 18 and 24 the higher C_{Chl} and C_{SPM} could be identified in the 2–4 m thick upper layer. The Chl *a* concentration was much higher in station 18 than in station 24, while the SPM concentrations were comparable. Thus, we may conclude that SPM in station 24 contained mainly mineral particles while comparable amounts of mineral and phytoplankton particles occurred in station 18.

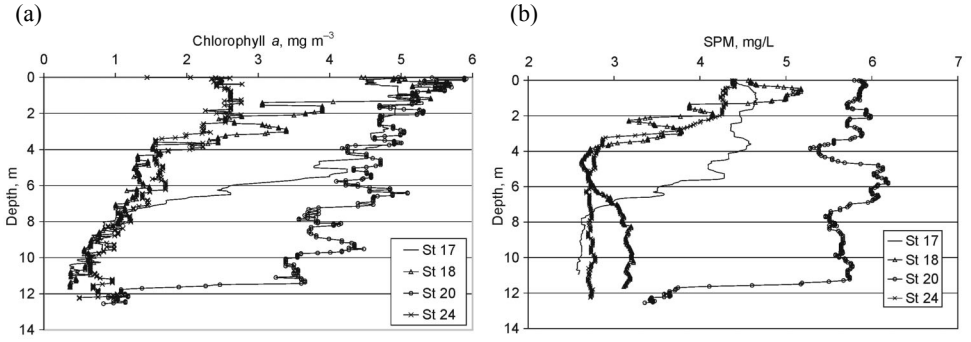

Fig. 3. (a) Vertical profiles of the calculated Chl *a* concentration in stations 17, 18, 20, and 24; (b) vertical profiles of the calculated SPM concentration in stations 17, 18, 20, and 24.

Optical properties affect biological production and vice versa. A widely used optical property is diffuse attenuation coefficient (K_d), which characterizes the gradient of vertical decrease of radiation in the water. We calculated K_d from the absorption and scattering coefficients of surface water data according to the formulas by Kirk (1994):

$$K_d = \frac{1}{\mu_0}\sqrt{a^2 + (0.425\mu_0 + 0.1092)ab}, \quad (4)$$

where μ_0 is the cosine angle of reflected photons just underneath the water surface, a is the absorption coefficient, and b is the scattering coefficient. The euphotic zone is defined as the layer in which the surface value of photosynthetically active region (PAR) is attenuated to the level of 1% of the incoming light (Tilzer, 1989). The depth of the euphotic zone, $z_{1\%}$, can be calculated as follows:

$$z_{1\%} \cong \frac{4.605}{K_d}. \quad (5)$$

The mean value of K_d for 412–715 nm and the corresponding euphotic depth are shown in Table 2. The K_d value varied between 0.87 and 1.23 and the depth of the euphotic zone was between 3.7 and 5.10 m. The euphotic zone was the shallowest in stations 17, 18, 20, and 24. The Chl *a* content showed a sharp decrease between the depths 4 and 6 m in the considered stations except in station 20. This result corresponds well with the depth of the euphotic layer.

Table 2. Calculated diffuse attenuation coefficient and the euphotic depth in the stations

Station	K_d(412–715)	$z_{1\%}$
16	0.90	5.10
17	1.07	4.32
18	1.14	4.04
19	0.94	4.92
20	1.23	3.73
21	0.87	5.32
22	0.91	5.04
23	0.90	5.10
24	1.05	4.41
25	0.97	4.74
26	0.92	5.03
27	0.96	4.78
28	0.95	4.87

The (active sensor) SAR measures the backscatter of microwave from the surface. The main factor that influences the backscatter from the sea is surface roughness due to Bragg waves (Heron & Prytz, 1996). Previous studies (Solberg et al., 2007) show that the most suitable wind speed for oil detection from SAR images is above 3 m s^{-1} as the Bragg wave field has fully developed in the case of this speed. Oil spills are detectable because of their dampening effect on Bragg waves, which leads to the reduction of microwave backscatter from the slick, therefore making the oil spill appear darker on the SAR image compared to the surrounding water. In addition to oil slick there are natural phenomena (local low wind area, algae, upwelling, internal waves, etc.) that appear as dark structures on the sea surface. Therefore, an important part of oil spill detection is separation of oil slicks from look-alikes.

The ASAR image from Muuga Bay on 30 May 2007 is shown in Fig. 4. Visual examination of the image indicated the presence of several dark structures. In the area covered by measurements the structures that can be identified as oil spills (based on the in situ measurements) were in the western coastal part of Muuga Bay. Also outside the measurement area the dark patches can be seen in the south-eastern part of the bay.

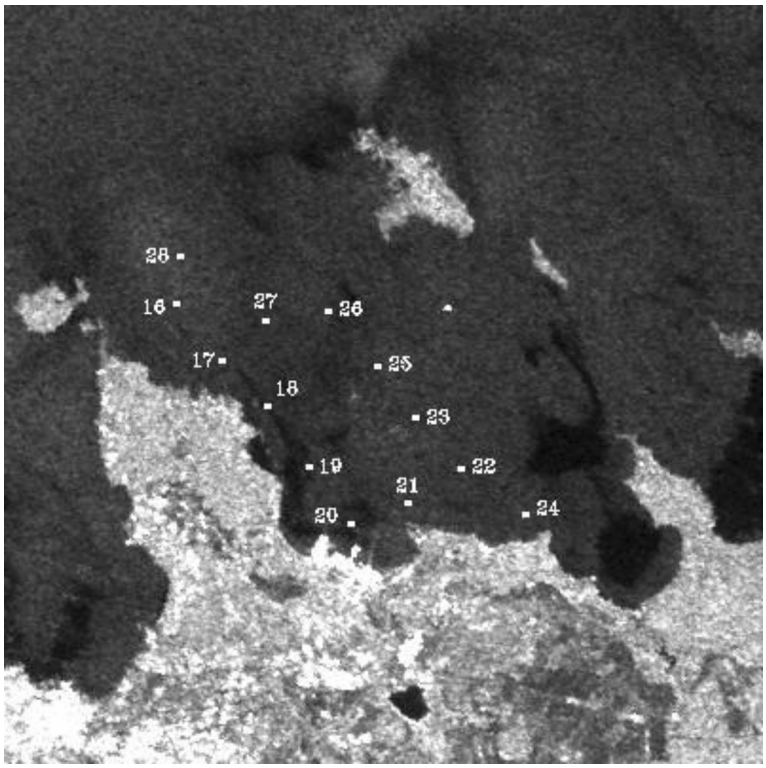

Fig. 4. Locations of stations on the Envisat ASAR Wide Swath image.

We examined the correlations between the ASAR data with surface temperature, Chl *a* concentration, SPM concentration, and the concentration of oil products in the sampled stations in Muuga Bay. The results of regression analysis are given in Table 3. Studies by Brekke & Solberg (2005) and Bentz et al. (2004) showed that the areas with lower sea surface temperature (SST) appear as dark areas on SAR images and can cause oil-spill look-alikes. Regression analysis of the SAR data and SST data showed no correlation ($R = 0.16$) between these parameters. For instance, the lowest temperature was measured in station 24, where water surface roughness (Bragg waves) is well developed (Fig. 4). Also, the organic

Table 3. Parameters of regression formulas between ASAR and field data

Regression	X variable	Intercept	*R*	*p*-Level	Samples	
ASAR vs Chl *a*	–0.01356	5.8696	0.34	0.0047	13	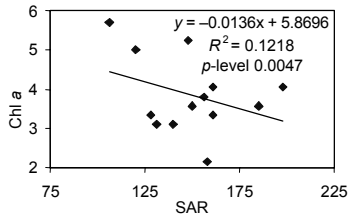
ASAR vs SPM	–0.02524	7.7851	0.64	0.000144	13	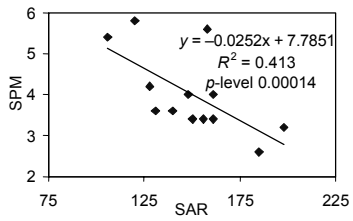
ASAR vs oil products	–0.0138	2.9306	0.71	0.013	8	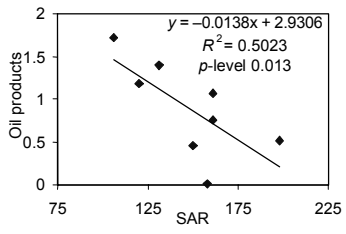
ASAR vs temperature	–0.0083	9.2697	0.16	0.0025	13	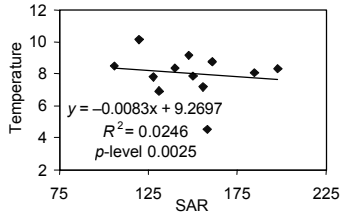

films caused by phytoplankton are a known source of look-alikes on SAR images (Brekke & Solberg, 2005; Bentz et al., 2004). Our data form Muuga Bay did not show high correlation (0.34) between SAR and Chl *a* content in water on 30 May 2007. Indeed, Chl *a* concentration was high in stations 17, 18, and 20, which are in or close to the areas of low SAR values. Still, no general correlation pattern with high Chl *a* and low SAR values could be detected. The correlation coefficient for SPM concentration and SAR data was 0.64. The SPM concentration was the highest in the stations where bilge water was detected during the measurements. This also explains the significant correlation between these parameters as bilge water contains residues of oil products and oil can be adsorbed on the surface of particulate matter. The highest correlation (0.71) was obtained between the oil products and SAR data although the concentration of oil products was relatively low (0.001–1.72 ppm) and the uncertainty level was not exceeded because of the small number of stations. The results show that weather conditions of that day enabled to detect even a small concentration of polluted water from the SAR image.

CONCLUSIONS

A case study of the spatial distribution of simultaneously obtained physical and inherent optical properties, optically active substances, and oil products and an ASAR image in Muuga Bay showed that the spatial variation was high even though the study area was relatively limited. The upwelling situation caused by the moderate wind from the east prevailed at the southern coast of the bay with low temperature, high salinity, high concentration of SPM, and low concentration Chl *a*. The western part of the bay was covered by warmer, less saline, and Chl *a* rich surface water, probably pushed towards the coast from the open bay area when the wind started to blow from the east. In general, higher concentrations of CDOM were detected at the stations that were located in the open part of the bay. At the Muuga harbour the water had high concentrations of SPM and Chl *a*, which caused a strong light attenuation and a thin euphotic layer compared to the other parts of the bay.

Regression analysis showed a significant correlation between the Chl *a* concentration and the absorption coefficient at 676 nm, and between the SPM concentration and the scattering coefficient at 555 nm. Analysis of the ratio of the absorption and scattering coefficients revealed that scattering was dominated over absorption almost in the whole spectral range in the stations with high concentrations of Chl *a* and SPM. The opposite was observed for the stations with low concentrations of Chl *a* and SPM, particularly for 412 nm wavelength.

Regression analysis between the measured parameters and SAR data gave the following results. One of the known look-alikes on SAR images is caused by upwellings. During our measurement day the eastern wind was pushing colder water to the south-eastern coastal stations. As a result, the measured temperature range of the surface water was 4.5–10.1 °C. However, regression analysis did not

show any correlation between temperature and SAR data on that day in Muuga Bay. There was no correlation between the Chl *a* and SAR data either. The correlation coefficient between SPM and SAR data was 0.64. The stations having a higher SPM concentration had smaller SAR backscattering values. High SPM concentrations were measured in stations where ballast water was visible on the water surface. The highest correlation (0.71) was obtained between the concentration of oil products and SAR data, although the concentration of oil products was relatively low – 0.001–1.72 ppm.

ACKNOWLEDGMENT

The work was supported by the Enterprise Estonia project 'Early detection and forecast of oil spill drift' (EU23689).

REFERENCES

Bentz, C. M., Lorenzzetti, J. A. & Kampel, M. 2004. Multi-sensor synergistic analysis of mesoscale oceanic features: Campos Basin, south-eastern Brazil. *Int. J. Remote Sens.*, **25**, 4835–4841.

Brekke, C. & Solberg, A. H. S. 2005. Oil spill detection by satellite remote sensing. *Remote Sens. Environ.*, **95**, 1–13.

Claustre, H., Fell, F., Oubelkheir, K. & Prieur, L. 2000. Continuous monitoring of surface optical properties across a geostrophic front: Biogeochemical inferences. *Limnol. Oceanogr.*, **45**, 309–321.

Erftemeijer, P. L. A. & Lewis, R. R. R. 2006. Environmental impacts of dredging on seagrasses: A review. *Mar. Pollut. Bull.*, **52**, 1553–1572.

Gade, M. & Alpers, W. 1999. Using ERS-2 SAR images for routine observation of marine pollution in European coastal waters. *Sci. Total Environ.*, **237**, 441–448.

Herlevi, A. 2002. Inherent and apparent optical properties in relation to water quality in Nordic waters. Academic dissertation in Geophysics. University of Helsinki.

Heron, M. L. & Prytz, A. 1996. Coherence scales for microwave Bragg scatter. In *OCEANS '96. MTS/IEEE. Prospects for the 21st Century. Conference Proceedings. 23–26 Sept. 1996*, Vol. III, 1400–1405.

Højerslev, N. K. 1980. On the origin of yellow substance in the marine environment. *Oceanogr. Rep. Univ. Copenhagen, Inst. Phys.*, 42, 1–35.

Kirk, J. T. 1994. *Light and Photosynthesis in Aquatic Ecosystems*. Cambridge University Press, Cambridge, New York.

Lorenzen, C. J. 1967. Determination of chlorophyll and phaetopigments; spectrophotometric equations. *Limnol. Oceanogr.*, **12**, 343–346.

McKee, D., Cannigham, A., Slater, J., Jones, K. J. & Griffits, C. R. 2003. Inherent and apparent optical properties in coastal waters: A study of the Clyde Sea in early summer. *Estuar. Coast. Shelf Sci.*, **56**, 369–376.

Sipelgas, L., Arst, H., Kallio, K., Erm, A., Oja, P. & Soomere, T. 2003. Optical properties of dissolved organic matter in Finnish and Estonian lakes. *Nord. Hydrol.*, **34**, 361–386.

Sipelgas, L., Arst, H., Raudsepp, U., Kõuts, T. & Lindfors, A. 2004. Optical properties of coastal waters of northwestern Estonia: in situ measurements. *Boreal Environ. Res.*, **5**, 447–459.

Sipelgas, L., Raudsepp, U. & Kõuts, T. 2006. Operational monitoring of suspended matter distribution using MODIS images and numerical modeling. *Adv. Space Res.*, **38**, 2182–2188.

Solberg, A. H. S., Storvik, G., Solberg, R. & Volden, E. 1999. Automatic detection of oil spills in ERS SAR images. *IEEE Trans. Geosci. Remote Sens. E.*, **37**, 1916–1924.

Solberg, A. H. S., Brekke, C. & Husoy, P. O. 2007. Oil spill detection in Radarsat and Envisat SAR images. *IEEE Trans. Geosci. Remote Sens.*, **45**, 746–755.

Tilzer, M. M. 1989. The productivity of phytoplankton and its control by resource availability. A review. In *Phycotalk* (Kumar, H. D., ed.), pp. 1–40. Bavaras Hindi University, Centre for Advanced Studies in Botany, Varanasi.

Topouzelis, K., Karathanassi, V., Pavlakis, P. & Rokos, D. 2007. Detection and discrimination between oil spills and look-alike phenomena through neural networks. *ISPRS J. Photogramm.*, **62**, 264–270.

Rannikumere optilised ja füüsikalised omadused ning nende seosed radari andmetega Muuga lahe näitel

Liis Sipelgas, Urmas Raudsepp ja Rivo Uiboupin

30. mail 2007 viidi Muuga lahe 13 mõõtejaamas läbi temperatuuri, soolsuse ja neeldumis- ning nõrgenemiskoefitsientide vertikaalsete profiilide mõõdistus. Määrati mõõtejaamades kogutud veeproovide üldnaftaproduktide, klorofülli *a*, heljumi ja lahustunud orgaanilise aine kontsentratsioon. Mõõtmiste läbiviimise päeval laaditi maha ja töödeldi ka radari ASAR kujutis Muuga lahe piirkonnast.

Regressioonanalüüs mõõdetud parameetrite vahel näitas, et klorofülli *a* kontsentratsioon korreleerub neeldumiskoefitsiendiga lainepikkusel 676 nm ja heljumi kontsentratsioon hajumiskoefitsiendiga lainepikkusel 555 nm. Leitud seoste põhjal arvutati heljumi ja klorofülli *a* vertikaalsed jaotused mõõtejaamades. Regressioonanalüüs üldnaftaproduktide ja radari andmete vahel andis korrelatsioonikoefitsiendi 0,71, mis näitab, et isegi väike kogus naftaprodukte vees vähendab tagasihajumist.